ture–Activity Relationships (Spencer, R. P., Ed.) Chapter 12, pp 251–266, Grune and Stratton, New York.
Pathak, M. S., Jimbow, K. Szabo, G., & Fitzpatrick, T. B. (1976) in *Photochemical and Photobiological Reviews* (Smith, K. C., Ed.) Vol. 2, pp 211–239, Plenum, New York.
Pines, A., Gibby, M. G., & Waugh, J. S. (1973) *J. Chem. Phys. 59*, 569–590.
Potts, A. M. (1964) *Invest. Ophthalmol. 3*, 405–416.
Pullman, A., & Pullman, B. (1961) *Biochim. Biophys. Acta 54*, 384–385.
Sarna, T., Froncisz, W., & Hyde, J. S. (1980) *Arch. Biochem. Biophys. 202*, 304–313.
Sealy, R. C., Hyde, J. S., Felix, C. C., Menon, I. A., Prota, G., Swartz, H. M., Persad, S., & Haberman, H. F. (1982a) *Proc. Natl. Acad. Sci. U.S.A. 79*, 2885–2889.
Sealy, R. C., Hyde, J. S., Felix, C. C., Menon, I. A., & Prota, G. (1982b) *Science (Washington D.C.) 217*, 545–547.
Stipanovic, A. J., Giammatteo, P. J., & Robie, S. B. (1985) *Biopolymers 24*, 2333–2343.
Strzelecka, T. (1982) *Physiol. Chem. Phys. 14*, 233–237.
Swan, G. A. (1963) *Ann. N.Y. Acad. Sci. 100*, 1005–1019.
Swan, G. A. (1974) *Fortschr. Chem. Org. Naturst. 31*, 521–582.
Thathachari, Y. T., & Blois, M. S. (1969) *Biophys. J. 9*, 77–89.
Vassallo, A. M., Wilson, M. A., Collin, P. J., Oades, J. M., Waters, A. G., & Malcolm, R. L. (1987) *Anal. Chem. 59*, 558–562.
Williams-Smith, D. L., Dunne, L. J., Evans, S., Pritchard, R. G., & Evans, E. L. (1976) *FEBS Lett. 69*, 291–294.

A Calorimetric Analysis of Human Plasma Fibronectin: Effects of Heparin Binding on Domain Structure†

Walter E. Niedzwiadek,‡ G. Thomas O'Bryan,‡ Frank A. Blumenstock,‡,§ Thomas M. Saba,*,§ and Thomas T. Andersen‡

Departments of Biochemistry and Physiology, Albany Medical College, Albany, New York 12208

Received October 21, 1987; Revised Manuscript Received May 24, 1988

ABSTRACT: Fibronectin domain structure, as influenced by interaction with heparin, calcium, or chondroitin sulfate C, was analyzed by differential scanning calorimetry. A complex thermal denaturation transition was observed with a large sharp endotherm at 63 °C, a broad endotherm between 70 and 80 °C, and an exotherm at 80–90 °C. Analysis of the denaturation profiles revealed the existence of four thermal transitions, 59.1, 62.2, 67.3, and 74.3 °C, and an exotherm at 83.9 °C. The calorimetric enthalpies of the four endotherms are 1146 ± 259, 866 ± 175, 1010 ± 361, and 676 ± 200 kcal/mol, respectively. In all cases, the calorimetric to van't Hoff enthalpy ratio was greater than 1.0. Computer analysis of the primary structure of fibronectin revealed 29 ± 8% homology among the type I homology units and 28 ± 7% homology among type III homology units, suggesting that different structural domains could arise from the same homology type. This may explain why more thermal transitions are observed for fibronectin than there are homology types. Addition of heparin to fibronectin in varying molar ratios, i.e., 10:1 to 30:1, resulted in a larger calorimetric enthalpy for the first type of structural domain (T_m = 59.1 °C) of fibronectin. At higher heparin to fibronectin ratios (40:1 or 75:1), the enthalpy of this domain decreased, while the others remained unchanged. In the presence of 5 mM calcium chloride, fibronectin thermal denaturation occurred at lower temperatures and was associated with precipitation of fibronectin. With both calcium chloride (5 mM) and heparin (20:1), a decrease in the total enthalpy of denaturation of fibronectin was observed, precipitation did not occur, and the T_m's were comparable to fibronectin in the absence of Ca^{2+}. Chondroitin sulfate C resulted in a large endotherm at 61.2 °C and aggregation above 65 °C, which was unlike the response to heparin. Thus, fibronectin has multiple heparin binding sites which differ in their affinities for heparin and sensitivity to calcium. These calorimetric assessments of the structural domains of fibronectin may provide insight into the structure–function relationships of the molecule.

Fibronectin is a large, adhesive, glycoprotein which exists in both plasma and tissue (Mosher, 1984; Ruoslahti et al., 1981). The concentration of fibronectin in human plasma is between 300 and 400 μg/mL (Mosesson & Umfleet, 1970). Plasma fibronectin is an opsonic molecule that promotes phagocytosis of nonbacterial particulates (Rourke et al., 1984). Fibronectin is also a component of the extracellular matrix and involved in wound healing and fibroblast adhesion to substratum (Saba, 1982; Yamada, 1983). Cell adhesion, cell–cell interaction, and integrity of the vascular barrier (Cohler et al., 1987) are promoted by fibronectin in tissues (Klebe et al., 1977; Kleinman et al., 1981; Yamada, 1983; Yamada & Olden, 1978). After trauma, burn, or starvation, the plasma fibronectin levels decrease in association with depression of reticuloendothelial phagocytic function (Deno et al., 1984; Saba, 1982; Saba et al., 1984), implying an important function for fibronectin in host defense following injury. While differences in primary structure exist between plasma and tissue fibronectin, the two forms are structurally very

† This study was supported by U.S. Public Health Service Grant GM-21447 from the Institute of General Medical Sciences and by an Institutional Biomedical Research Support grant. The purified human fibronectin was provided by Rorer, Inc., Fort Washington, PA.

* Address correspondence to this author at the Department of Physiology, Albany Medical College, 47 New Scotland Ave., Albany, NY 12208.
‡ Department of Biochemistry.
§ Department of Physiology.

0006-2960/88/0427-7116$01.50/0

similar and differ only slightly antigenically (Click & Balian, 1985; Hayashi & Yamada, 1981).

On the basis of the sequence analyses of Kornblihtt et al. (1985) and assuming a carbohydrate content of 5.1% (Mosesson et al., 1975), plasma fibronectin has a molecular weight of approximately 540000 and is composed of two nearly identical polypeptide chains joined near the C-terminus by a pair of disulfide bonds (Akiyama & Yamada, 1987; Hynes, 1985; Yamada, 1983). The primary structure for human plasma fibronectin, based on the cDNA sequence data of Kornblihtt et al. (1985), is very homologous with the primary structure of bovine plasma fibronectin as derived from peptide sequencing studies (Skorstengaard et al., 1986). Little is known about the higher order structures of fibronectin, but the intact molecule does contain several functional regions which have the ability to bind ligands such as fibrinogen, fibrin (Hormann & Seidl, 1980), collagen (Jilek & Hormann, 1979), actin (Keski-Oja & Yamada, 1981), heparin, or hyaluronic acid (Yamada et al., 1980). It is not clear if the functional regions of fibronectin comprise discrete structural domains, or if multiple structural domains interact to form a functional (binding) region. Such information would be important in attempts to generate smaller portions of fibronectin with a particular biological function for potential therapeutic value.

Heparin added to plasma results in enhanced cryoprecipitate formation at 4 °C (Thomas et al., 1954). Calcium and sodium as well as the pH of the solution can influence the amount of heparin-induced cryoprecipitate formed (Stathakis & Mosesson, 1977). Increasing calcium ion concentrations (0–7.5 mM) increase cryoprecipitate formation while increasing sodium ion concentrations (74–250 mM) or raising the pH (7–9) decrease cryoprecipitate formation. Heparin binds to fibronectin (Yamada et al., 1980) and increases the ability of fibronectin to bind collagen (Jilek & Hormann, 1979; Johansson & Hook, 1980). Some of the heparin binding areas are reported to be near the collagen binding area (Petersen et al., 1983).

Differential scanning calorimetry is a powerful method with which to examine the domain structure of a molecule in either a qualitative or a quantitative sense (Privalov, 1982). It can also be used to examine how structural domains are affected by binding of ligands (Fukada et al., 1983). We employed calorimetry to characterize the domain structure of human plasma fibronectin in a quantitative, thermodynamic manner, and to monitor the effects of heparin and other ligands on the structural domains of fibronectin. We did not measure the enthalpy of binding of ligands to fibronectin, but rather the change in enthalpy after ligand binding for the thermal denaturation of structural domains of fibronectin.

Materials and Methods

Human plasma fibronectin, purified under sterile conditions by gelatin–Sepharose affinity chromatography using fibronectin-rich plasma cryoprecipitate derived from a defined healthy donor population as the source of material (Saba et al., 1986), was provided as a lyophilized powder (Rorer, Inc., Fort Washington, PA). Sucrose, Tween 80 detergent, sodium citrate, sodium chloride, and potassium hydroxide were obtained commercially (Fisher Scientific, Fairlawn, NJ). Heparin (porcine intestinal mucosa; assumed average molecular weight 13000; sodium salt form; activity of 162 units/mg, lot 66F-0727) and chondroitin sulfate C (shark cartilage; assumed average molecular weight 29000; sodium salt, lot 70F-0606) were obtained commercially (Sigma Chemical Co., St. Louis, MO). A heparin solution (9.50 mM) was prepared by dissolving 185 mg of heparin to a final volume of 1.5 mL of buffer. A calcium chloride solution was prepared in buffer to a final concentration of 710 mM.

Prior to use, distilled water was added to the lyophilized, purified fibronectin. After reconstitution, the fibronectin solution contained 5% sucrose, 0.05% Tween 80, 2 mM sodium citrate, 75 mM sodium chloride, and 5 mg/mL fibronectin. A comparable diluent buffer solution (5% sucrose, 0.05% Tween 80, 2 mM sodium citrate, and 75 mM sodium chloride) at pH 7.4 was used for the reference cell and for solutions of heparin, Ca^{2+}, and other ligands. The concentration of fibronectin was determined with a Perkin-Elmer 320 recording spectrophotometer, path length 1 cm, using an extinction coefficient of 1.28 mL/(mg·cm) at 280 nm (Mosesson & Umfleet, 1970).

A MC-1 differential scanning calorimeter (Micro Cal, Inc., Amherst, MA), modified for analog output to a computer, was used along with an IBM personal computer equipped with a DT2801 analog-to-digital converter (Data Translation, Inc., Marboro, MA) and an 8087 math coprocessor chip. Data acquisition and analysis software, DA-2, were purchased from Micro Cal., Amherst, MA.

Calorimetric measurements were performed using a heating rate of 1 °C/min and a protein concentration of 5 mg/mL. The Hastalloy cells had a volume of 0.9 mL and contained 0.70 mL of the protein solution (3.5 mg of fibronectin) or 0.70 mL of buffer. The loaded cells were equilibrated under vacuum (usually 20–40 min), and air was then let into the apparatus to a pressure of 10–15 mmHg. Data were collected, using the DT2801 board, during 25-s intervals, averaged, and displayed. From these data, the thermodynamic quantities were determined by using the DA-2 deconvolution software (Freire & Biltonen, 1978a,b,c).

Immediately after scanning, the contents of the sample and reference cells were removed, and the cells were cleaned with 80 mL of 0.5 M KOH heated to 85 °C into which the cells were immersed for 15 min. Each cell was then washed thoroughly with 500 mL of 2% Micro cleaner (American Scientific Products, Edison, NJ) in distilled water heated to 85 °C and rinsed with 1000 mL of 85 °C distilled water. The cells were cooled to room temperature and placed under vacuum for 15–20 min to remove remaining moisture prior to being loaded for the next scan.

For ligand studies, heparin was added to both the sample and reference cells of the calorimeter. In the sample cell, the molar ratio of heparin to fibronectin ranged from 10:1 to 75:1 (6.8 μL of heparin added to give a 10:1 molar ratio, weight ratio 0.24 mg of heparin/mg of fibronectin). A calorimetric scan of heparin (using an amount of heparin equivalent to a 100:1 molar ratio) was performed in the absence of fibronectin and resulted in no detectable signal (data not shown). Calcium chloride was added to both cells, in the presence or absence of heparin, to give a final concentration of 5 mM calcium (5.0 μL of calcium chloride to obtain a final concentration of 5 mM). We accounted for the volumes of both the calcium chloride and heparin solutions in determining the final concentration.

Fibronectin sequence homology within the three reported homology types was evaluated and displayed graphically using a PHAST (protein homology analysis software) program developed in this laboratory. Two different segments of the primary sequence of fibronectin, which were of the same homology type, were placed on the abscissa and ordinate, starting at the upper left corner of the graph (Figure 1). The analysis compared each amino acid residue along the abscissa to each residue of the ordinate, locating all identical residues

Table I: Homology within Type I Homology Units[a]

	1	2	3	4	5	6	9	10	11	29	30	31
1	100	27	29	36	30	34	34	28	32	25	26	28
2		100	34	50	31	27	36	34	31	25	15	20
3			100	39	44	31	44	41	36	19	30	20
4				100	34	34	36	34	34	21	23	26
5					100	29	38	34	38	20	15	17
6						100	40	28	29	14	17	31
9							100	41	38	12	28	22
10								100	34	17	17	24
11									100	20	17	22
29										100	36	31
30											100	40
31												100

[a] The homology units were aligned according to Petersen et al. (1983), and homology is reported as the percent of total residues that are identical. Identifying numbers represent names (line numbers in Figure 2) for the individual type I homology units in the order that they are found in the primary structure of fibronectin.

Table II: Homology within Type III Homology Units[a]

	12	13	14	15	16	17	18	19	20	21	22	23	24	25	26
12	100	23	22	21	18	11	17	21	27	23	26	20	27	23	25
13		100	35	28	27	16	23	29	31	25	30	30	27	27	24
14			100	34	35	14	31	32	37	33	36	32	35	33	34
15				100	33	19	26	35	37	31	35	33	36	29	31
16					100	16	33	28	39	26	30	32	38	24	36
17						100	8	17	10	11	13	14	17	16	14
18							100	29	32	28	35	27	27	31	29
19								100	37	22	29	33	37	27	35
20									100	28	35	37	33	32	41
21										100	29	30	29	33	35
22											100	38	39	36	37
23												100	34	27	39
24													100	29	36
25														100	33
26															100

[a] The homology units were aligned according to Petersen et al. (1983), and homology is reported as percent of total residues that are identical. Numbers 12–26 are names (line numbers in Figure 2) assigned to individual type III homology units in the order that they are found in the primary structure of fibronectin.

(Krystek et al., 1985). For visual clarity, Figure 1 displays a mark for each residue when two or more adjacent identical residues occur in the sequence. A diagonal line indicates that significant homology exists. The software then calculated percent homology, using *all* identical residues, and this information was used to generate tables of homology.

Results

Sequence homology was examined within the three reported (Petersen et al., 1983) homology types of fibronectin in order to determine the extent to which different structural domains may arise from the same homology type. Figure 1 shows a representative comparison of the extent of homology within each type. Homology was maximized by aligning the sequences according to the convention of Petersen et al. (1983), as shown in Figure 2. A comparison is presented in Table I of the extext of homology among each of the various type I units, while Table II shows comparable data for the type III units. The amount of homology within each homology type is summarized in Table III. This analysis indicated that, while the sequence homology (Dayhoff et al., 1983) within type I units or within type III units is appreciable and may be significant from an evolutionary argument, any individual unit is more different from the other units within its type than it is alike (Table III). Thus, various units within a homology type may give rise to dissimilar structural domains. It should be emphasized that, in the current study, portions of the fibronectin sequence are being compared only to other portions within the same homology type. Sequences from different homology types are not compared to one another because of differences in length and in composition which necessarily result in distinct structural features.

Table III: Homology within Structural Domain Types

type	homology	range
I	29.2 ± 8.4	12–50
II	50.0	
III	28.4 ± 7.6	8–41

Table IV: Thermodynamic Parameters of Fibronectin Denaturation[a]

transition	T_m (°C)	ΔH_{cal} (kcal/mol)	ΔH_{vH} (kcal/mol)
1	59.1 ± 0.4	1146 ± 259	128 ± 17
2	62.2 ± 0.4	866 ± 175	133 ± 16
3	67.3 ± 2.3	1010 ± 361	65 ± 20
4	74.3 ± 1.0	676 ± 200	114 ± 44
exotherm	83.9 ± 3.4		

[a] The results are the mean ± SD of six repeat assays. The plasma fibronectin concentration of the test solution was approximately 5 mg/mL. A scan rate of 1 °C/min was employed.

Differential scanning calorimetry was applied to fibronectin at pH 7.4 over the temperature range 30–100 °C, and thermal denaturation profiles were obtained (Figure 3). Fibronectin had a major endotherm centered near 63 °C, a broad shoulder centered at 75 °C, and an exotherm occurring near 84 °C. The fibronectin denaturation transition was irreversible, even if heated only to 63 °C first and then rescanned after being cooled (data not shown).

To yield further information about the domain structure of fibronectin, the data were analyzed using the statistical mechanical deconvolution methods of Freire and Biltonen

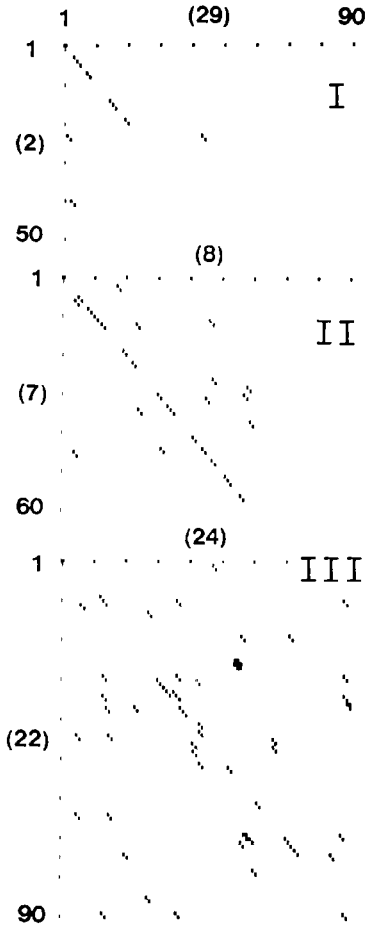

FIGURE 1: Homology comparison between segments of fibronectin of the same homology type. (I) Type I homology units, 2 vs 29; (II) type II homology units 7 and 8; (III) type III homology units, 22 vs 24. Numbers refer to sequences listed in Figure 2 and in Tables I and II.

Table V: Total Enthalpy as a Function of Heparin Concentration

molar ratio	heparin concn (mg of heparin/mg of fibronectin)	enthalpy (kcal/mol)
0	0	3698
10	0.24	3650
20	0.48	3529
30	0.72	4288
40	0.96	3860
75	1.80	3449

(1978a,b,c). Thermal denaturation profiles were fit to transitions whose thermodynamic parameters are listed in Table IV. The sum of these fit transitions is superimposed on the original scan (Figure 3), and although the fit is satisfactory for a molecule as complex as fibronectin, we would have more confidence in fitting transitions for isolated domains. This is currently in progress. The calorimetric to van't Hoff enthalpy ratios were large for each of the fit transitions of fibronectin.

A calorimetric scan of fibronectin in the absence and presence of heparin is shown in Figure 4. The upper curve shows fibronectin in the absence of ligand (as in Figure 3) while the lower curve shows fibronectin in the presence of a 40:1 molar ratio of heparin to fibronectin (weight ratio 0.96 mg of heparin/mg of fibronectin). Changes caused by the interaction of heparin with fibronectin include a shift in the main endotherm T_m around 60 °C and a more pronounced shoulder around 70 °C. The change in enthalpy of the transitions with increased heparin dose is shown in Figure 5. The first thermal transition experienced the greatest amount of change due to heparin, while the second and third were affected to a lesser extent. The fourth thermal transition was unaffected by heparin. The calorimetric enthalpies of the four transitions were summed for each of the heparin doses as displayed in Table V. The total enthalpy remains fairly constant over the heparin dose range used with a small increase at a heparin to fibronectin molar ratio of 30:1.

FIGURE 2: Primary structure of human fibronectin. The sequence is displayed to give maximum homology between segments of fibronectin. *ED* refers to the "extra domain" present in some forms of fibronectin; *CS* refers to an area where the two chains of fibronectin vary. Dashed lines indicate pairing of cysteine residues to form disulfides (which is conserved for each unit within a homology type). The sequence is from Kornblihtt et al. (1985), and homology types are based on the convention of Petersen et al. (1983).

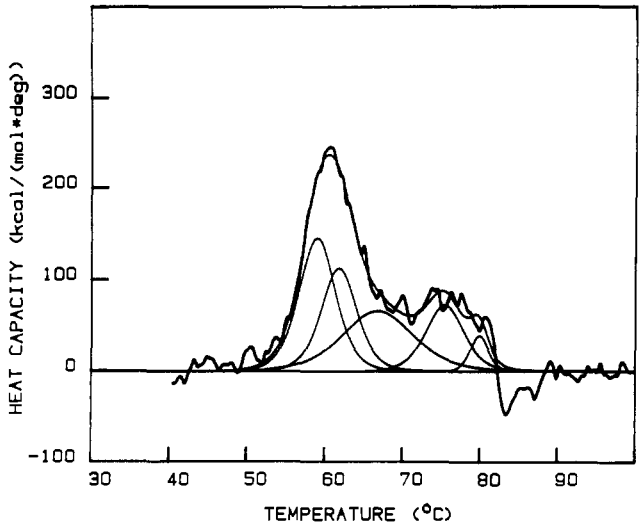

FIGURE 3: Thermal denaturation profile of fibronectin. Fibronectin was scanned using the differential scanning calorimeter at a temperature increment rate of 1 °C/min between 30 and 100 °C. The computer-fit curve (smooth line) is superimposed on the actual data trace (line with variation). The computer-fit curve is the sum of five individual transition curves displayed beneath the actual data trace. The fifth curve (far right) was included in the composite curve even though it had a calorimetric to van't Hoff enthalpy ratio less than 1. It was excluded from analysis in Table IV. The base line was established according to Jackson and Brandts (1970).

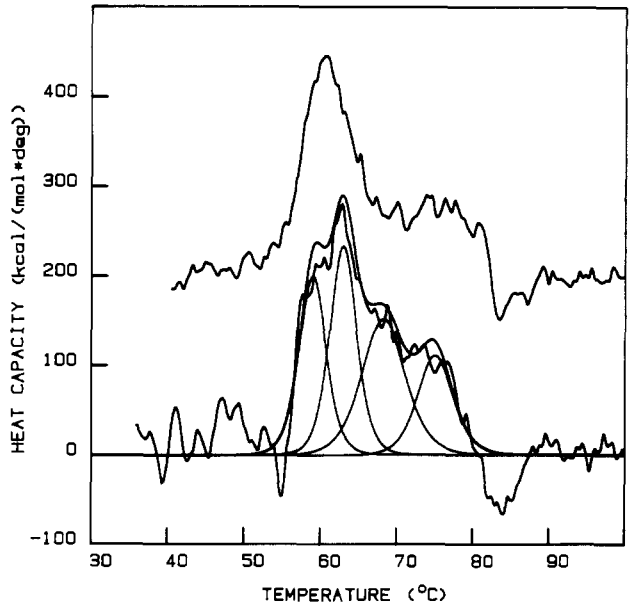

FIGURE 4: Thermal denaturation profile of fibronectin in the absence (top curve) and presence (bottom curve) of heparin. A 40:1 molar ratio of heparin to fibronectin was scanned using differential scanning calorimetry at a temperature increment rate of 1 °C/min between 30 and 100 °C. The computer-fit curve (bold smooth line) is superimposed on the actual data trace (bold line with variation) and is the sum of the four individual transition curves (thin smooth lines) displayed beneath the actual data trace.

As a control for heparin, chondroitin sulfate C was added to fibronectin at a molar ratio of 20:1. The differential calorimetric scan is shown in Figure 6. Analysis of the data reveals a transition occurring at 61.2 °C. Above 65 °C, an erratic trace was detected, which corresponded to formation of a precipitate clearly detectable after the calorimetric scan was complete. No such precipitate was formed when chondroitin sulfate C or fibronectin was scanned alone or when fibronectin was scanned in the presence of heparin.

Calcium has been reported to inhibit the binding of heparin to fibronectin fragments (Hayashi & Yamada, 1982). In order

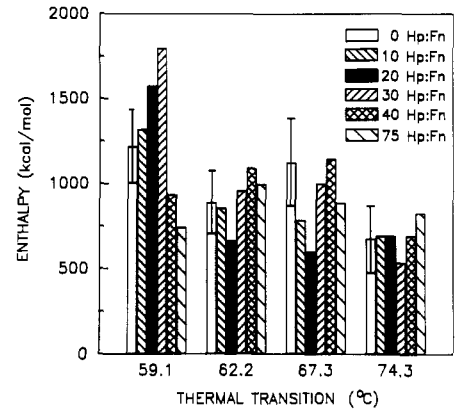

FIGURE 5: Effect of heparin on the calorimetric enthalpy (ΔH_{cal}) of fibronectin during thermal denaturation. The zero heparin dose is on the left in each group with increasing heparin doses to the right. The error bars indicate the standard deviation about the mean for the zero heparin dose ($n = 5$) at each temperature. Duplicate samples were used for all other studies. Numbers on the abscissa are the T_m's for the four transitions displayed graphically in Figure 4.

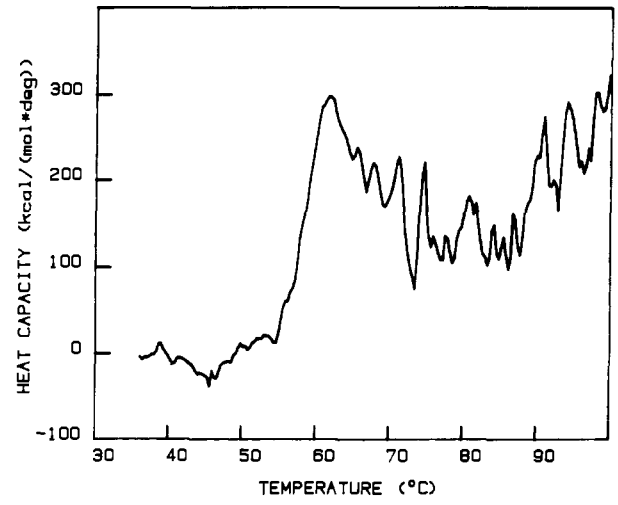

FIGURE 6: Thermal denaturation profile of fibronectin in the presence of chondroitin sulfate C. Chondroitin sulfate C, a highly charged polysaccharide, was used as a control for heparin in a 20:1 molar ratio. It was scanned between 30 and 100 °C, the data trace became erratic, and a precipitate was formed.

to investigate what effect calcium ions, which are a component of the in vivo plasma environment of soluble fibronectin (Ryder et al., 1975), may have on the structural domains of fibronectin, 5 mM calcium chloride was added to fibronectin, and the mixture was scanned at 1 °C/min. Figure 7A shows the differential calorimetric scan of fibronectin in the presence of $CaCl_2$. A major endotherm was seen centered around 60 °C with the transition occurring between 50 and 65 °C. After 65 °C, the calorimetric scan was erratic, and a white, flocculent precipitate was observed after the denaturation process was complete, much like that seen for chondroitin sulfate C.

When both calcium (5 mM) and heparin (20:1 molar ratio, 0.18 mM) were added to fibronectin (Figure 7B), no aggregation or precipitation of fibronectin was observed, suggesting that heparin may reverse some of the effects of calcium on fibronectin and that calcium does not prevent the binding of heparin to fibronectin.

Discussion

Differential scanning calorimetry of fibronectin yielded a large, sharp endotherm near 63 °C, a broad endotherm between 70 and 80 °C, and an exotherm at 80–90 °C. The transitions are irreversible after being scanned and are also

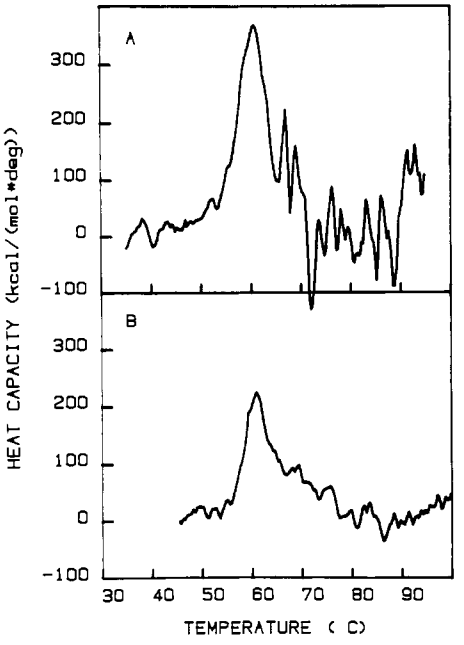

FIGURE 7: Thermal denaturation profiles of fibronectin in the presence of calcium (A) or calcium + heparin (B). (A) Fibronectin in the presence of 5 mM calcium chloride. (B) Fibronectin in the presence of 5 mM calcium and a molar excess of heparin to fibronectin of 20:1. The concentration of heparin is 0.18 mM. The erratic nature of the calorimetric scan for fibronectin denaturation in the presence of calcium above 65 °C is seen clearly (panel A). This aggregation process was eliminated when heparin was present (panel B).

irreversible if heated to 63 °C first, then cooled, and rescanned. This calorimetrically detected irreversibility correlates with the previously reported loss of fibronectin-related opsonic activity in serum heated to 60 °C (Saba et al., 1966). The data compare favorably with other physical studies (Alexander et al., 1979, 1978) of fibronectin, and the "irreversibility" of so complex a molecule is not unexpected (Manly et al., 1985). The exotherm between 80 and 90 °C suggests that fibronectin forms aggregates after thermal denaturation (Sturtevant, 1974). The exotherm observed for fibronectin varies by ±3.4 °C, which is large compared to the change in the T_m of the endotherms for each of the fit thermal transitions, reflecting the somewhat more random events of aggregation as compared to denaturation of a structural domain. The aggregates apparently are not large enough to precipitate because no precipitate was observed after the denaturation process was complete. Proteins can interact to form aggregates in many ways, whereas folding (or unfolding) is likely to follow a greatly restricted pathway (Go, 1983). Each subunit of fibronectin has two self-association sites, one near the N-terminus and a second near the C-terminus (Ehrismann et al., 1982). Thus, as fibronectin undergoes thermal denaturation, these sites from different molecules may interact, leading to aggregate formation, which would be an exothermal process (Sturtevant, 1974). The nature of the fibronectin thermal denaturation profile indicates qualitatively that fibronectin is composed of several different structural domains as suggested by Ruoslahti et al. (1981), which have distinct thermal denaturation transitions. Whether each structural domain undergoes a two-state denaturation process as suggested for other proteins (Ploplis et al., 1981; Privalov et al., 1981) remains to be determined.

Four transitions were resolved by deconvolution analysis of the fibronectin thermal denaturation profile (Figure 3). However, even these fit transitions are not likely to represent individual structural domains. Instead, several structural domains of fibronectin which denature with a similar T_m are likely to be contributing to each fit transition. This interpretation implies that multiple copies of each structural domain may be present, an interpretation which is consistent with the primary structure of fibronectin. Portions of the primary structure are reported to repeat in three different forms (Figure 2), referred to as homology types I, II, and III (Petersen et al., 1983). Since the primary structure of a protein dictates the way that the protein folds and forms higher order structures, it follows that repeating units of primary structure may result in multiple copies of different structural domains.

If the various homology types (I, II, and III) were highly conserved units of sequence identity, we would have expected to see three structural domains in the calorimetric assessment. However, the homology between fibronectin segments within a so-called "homology type" is only 8–50% (Figure 1, Tables I–III). The existence of homology within regions of fibronectin is appreciable but is defined more by certain conserved amino acid residues (e.g., half-cystine, tyrosine, or tryptophan) than by conserved stretches of sequence. Type I and II homology regions are defined by four conserved half-cystine residues, but the other residues in the units vary considerably. Similarly, type III regions are defined by aligned tyrosine and tryptophan residues, but here again, there is little homology among the remaining portions of these sequences. One might anticipate that there may be more than a single type of structural domain represented among the type III homology units.

We cannot definitively assign a particular thermal transition to a particular homology type. Type III homology regions may be expected to contribute most to the total enthalpy of the thermal denaturation profile because they constitute most (66%) of the primary structure of fibronectin. Type I and type II regions would contribute less to the total enthalpy because they make up only 26% and 5%, respectively, of the protein. The 59.1 and 62.2 °C transitions together constitute 54.4% of the total enthalpy while the 67.3 and 74.3 °C transitions constitute 27.3% and 18.3%, respectively. Furthermore, each type I and II homology unit has two disulfide bonds, while type III has none, and disulfides may be expected to impart greater thermal stability (i.e., higher T_m). On the basis of fluorescence data, Ingham et al. (1984) suggested that the N-terminal fragments (type I) were the most stable. For these reasons, we propose that the thermal transitions occurring at 59.1 and 62.2 °C are due to type III homology regions while those at 67.3 and 74.3 °C may be due to type I and II, though it is not yet possible to speculate which is type II and which is type I. This model ignores any contribution from the unclassified regions of the primary structure of fibronectin (those portions which connect the homology units), but this approximation seems justified in view of the small amount of the primary structure contributed by those connecting segments. While speculative, this model may be tested by calorimetric studies of fibronectin fragments. Thermal denaturation profiles of fragments which contain a single homology type would likely yield transitions with a calorimetric to van't Hoff enthalpy ratio of 1, as expected for a structural domain experiencing a two-state transition (Jackson & Brandts, 1970; Privalov, 1979).

This current analysis extends previous calorimetric observations on fibronectin (Koteliansky et al., 1981; Wallace et al., 1981). Previously, studies have indicated that changes which occur around 60 °C affect the function of the molecule (Wallace et al., 1981). To our knowledge, the first reported differential scanning calorimetry experiments done on fibronectin show that the protein unfolds between 45 and 70 °C with a maximum excess heat capacity at 65 °C and a calorimetric enthalpy of 2855 kcal/mol (Koteliansky et al., 1981).

These authors reported that six transitions existed. However, they did not present the calculated T_m and enthalpy values for the transitions. Therefore, although this previous study is in qualitative agreement with our current results, they cannot be compared quantitatively. Another differential scanning calorimetry study monitored fibronectin denaturation up to 135 °C with a scan rate of 10 °C/min and found three thermal transitions, 68, 82, and 119 °C, with calorimetric enthalpies of 1404, 216, and 378 kcal/mol, respectively (Wallace et al., 1981). Unlike our experiment in which fibronectin was in solution, this study used dry fibronectin sealed in a reaction pan. When these authors scanned fibronectin at 2 °C/min, the T_m of the first two transitions dropped to 62 and 76 °C, respectively, which is not unlike our findings using a scan rate of 1 °C/min. We did not examine the existence of any transitions at temperatures in excess of 100 °C and are therefore unable to comment on the transition previously reported to occur at 119 °C (Wallace et al., 1981). However, its detection may reflect the fact that the protein was not in solution. Variations in observed enthalpies between various laboratories may be due to differences in buffer systems utilized or the state of the protein (wet or dry) when analyzed.

Calcium chloride has been shown to decrease the ability of the N-terminal 31 000 molecular weight fragment of fibronectin to bind heparin (Hayashi & Yamada, 1982). The binding of heparin to this fragment is inhibited by 50% at 3–4 mM calcium chloride. Heparin binding to intact fibronectin decreased as the pH and ionic strength were raised (Bentley et al., 1985). Therefore, it seems reasonable to study heparin effects on fibronectin in the presence and absence of calcium since calcium may be of physiological importance to the interactions that fibronectin has with molecules in plasma (Ryder et al., 1975).

Electron spin resonance studies (Ankel et al., 1986) showed that addition of heparin or dextran sulfate induced a conformational change in fibronectin but chondroitin sulfates did not. Ankel et al. (1986) suggested that binding of heparin or dextran sulfate to fibronectin changes the molecular conformation of fibronectin to a more flexible state while chondroitin sulfates do not have this effect. Chondroitin sulfates do not bind to fibronectin (less than 1% of added chondroitin sulfates were bound) and cannot displace heparin or hyaluronic acid from fibronectin (Yamada et al., 1980).

Fibronectin can bind to actin and collagen, but these proteins have thermal transitions near those manifested by fibronectin. Non-protein ligands, such as heparin, offer a good alternative approach to probing the structure–function relationships of fibronectin by calorimetric studies. Heparin has been shown to bind to intact fibronectn with a K_D of 10^{-7}–10^{-8} M. Bound heparin cannot be displaced with hyaluronic acid, another ligand which binds to fibronectin with a K_D of 10^{-7} M (Yamada et al., 1980). At least two sites with different affinities for heparin are present in fibronectin, and only one site for hyaluronic acid is known. Thus, chondroitin sulfates can serve as a valuable control for heparin effects on fibronectin, since nonbinding effects such as ionic strength or pH changes can be monitored.

Heparin enhances the affinity of fibronectin for both native and denatured collagen (Jilek & Hormann, 1979). Chondroitin sulfate does not alter the affinity of fibronectin for collagen (Johansson & Hook, 1980). Heparin binding to fibronectin produced marked changes in the calorimetric scan, which included a variable exotherm, a broadening of the main endotherm at 60 °C, and a rise in the endotherm between 70 and 80 °C (at a 40:1 molar ratio). The difference between the peak heights of the two endotherms was noticeably less than the difference seen with fibronectin in the absence of heparin (Figure 4), due mostly to the increase in the higher temperature region. The total combined calorimetric enthalpy of the four thermal transitions (Table V) reached a maximum at a heparin to fibronectin ratio of 30:1 with a 16% increase from that in the absence of heparin. Although small, the amount of change was remarkable, considering that only a small portion (the binding region) of fibronectin was in contact with heparin. However, at higher heparin doses, the enthalpy decreased (Table V). In contrast, heparin did not appear to stabilize fibronectin as detected by fluorescence analysis (Ingham et al., 1984). These differences may be due to variations in the amount of heparin utilized. Thus, the binding of heparin may impart a stabilizing effect to the structure of fibronectin.

In the current study, we quantified the enthalpy change of each thermal transition of fibronectin in the presence of heparin and observed that heparin affects the 59.1 °C transition more than the others. Since heparin binding sites are reported to be in type III homology units (Figure 2), the observation is in keeping with our speculative model. The calorimetric enthalpy of the first thermal transition, T_m = 59.1 °C, steadily increased with increasing doses of heparin (between 10:1 and 30:1 molar ratios) to a maximum of 57% over the mean enthalpy value for fibronectin in the absence of heparin. However, increasing the heparin dose to 75:1 drastically reduced the enthalpy by 35% as compared to that observed in the absence of heparin. One possible explanation for this response is that at low heparin doses a single heparin molecule binds simultaneously to similar sites on each chain of fibronectin, i.e., spanning both subunits, which results in higher calorimetric enthalpy values. In contrast, at higher doses of heparin, the heparin binding sites on each of the fibronectin subunits may bind a different molecule of heparin. This may increase the stability of the individual structural domains but decrease the stability of the whole complex because the two chains of fibronectin interact with each other to a lesser extent, due to steric effects, as compared to that observed either in the absence of heparin or in the presence of a small amount of heparin. The findings by Bentley et al. (1985) would support this model for the interaction of heparin with fibronectin.

No difference in the thermal denaturation profiles could be detected for fibronectin in the presence of chondroitin sulfate C between 55 and 65 °C. However, above 65 °C, the calorimetric scan became very erratic, and a white, flocculent precipitate was formed. The results support the observations of Ankel et al. (1986) and Yamada et al. (1980) that chondroitin sulfate does not bind to intact fibronectin but it does influence denatured fibronectin.

One explanation for this effect may be that as the protein denatures and exposes hydrophobic residues, its chemical potential is increased, though not enough to cause precipitation. However, when the highly charged chondroitin sulfate is present, the chemical potential of the protein is increased still further, and phase separation (i.e., precipitation) occurs. This does not happen in the presence of highly charged heparin, but since heparin binds to fibronectin, it may counteract the large increase in chemical potential. A second but less attractive possibility is that as fibronectin is denatured, a cryptic binding site for chondroitin sulfate C could be made accessible, resulting in an interaction leading to precipitation. If this were the case, the binding of chondroitin sulfate C to fibronectin would be a temperature-dependent phenomenon not previously detected because the assays used to assess the binding of lig-

ands to fibronectin were carried out at or below room temperature (Yamada et al., 1980; Sekiguchi et al., 1983).

We also observed that the structural domains of fibronectin underwent changes in the presence of calcium ions. These changes resulted in the loss of thermostability of fibronectin at temperatures higher than 65 °C, but the protein appeared to have a thermal transition near 55 °C. Divalent ions such as calcium, magnesium, and manganese can result in the stabilization of a second structural domain of prothrombin (Ploplis et al., 1981). It may be that a similar situation exists for fibronectin. Calcium may stabilize a domain that was not apparent in the absence of divalent cation. It is less likely that calcium destabilizes a domain which denatures at a higher temperature in the absence of Ca^{2+}. A major exotherm was seen at 72 °C, perhaps reflecting aggregation as noted by the appearance of a precipitate after the denaturation process was complete.

In the current study, we also added both calcium and heparin to fibronectin (Figure 7) in order to assess the effects of calcium on the calcium-sensitive heparin binding regions (Hayashi & Yamada, 1982) of fibronectin. Addition of heparin to fibronectin in the presence of calcium resulted in a calorimetric scan that was smooth after the main endotherm with no precipitate observed (Figure 7, panel B). The height and width of the main endotherm were reduced, and the total enthalpy was less than that seen for fibronectin in the absence of either ligand. Analysis of the endotherm shows that it was composed of a transition at 60.8 °C with other transitions found at 68.9 and 75.6 °C. There was no indication of a lower T_m (55 °C) thermal transition for the calcium–heparin–fibronectin mixture.

Thus, the domains in fibronectin interact with each other, and the stability of one domain is dependent on the others. Heparin stabilizes the molecule and prevents precipitation upon heat denaturation. The total enthalpy of fibronectin decreased with both calcium and heparin present, perhaps because calcium prevented heparin binding to calcium-sensitive heparin binding regions. At the same time, heparin was able to bind to the calcium-insensitive binding regions. Thus, the added structural stability of fibronectin due to heparin binding appears largely mediated by calcium-sensitive heparin binding sites.

REFERENCES

Akiyama, S. K., & Yamada, K. M. (1987) *Adv. Enzymol. Relat. Areas Mol. Biol. 59*, 1–57.

Alexander, S. S., Jr., Colonna, G., Yamada, K. M., Pastan, I., & Edelhoch, H. (1978) *J. Biol. Chem. 253*, 5820–5824.

Alexander, S. S., Jr., Colonna, G., Yamada, K. M., & Edelhoch, H. (1979) *J. Biol. Chem. 254*, 1501–1505.

Ankel, E. G., Homandberg, G., Tooney, N. M., & Lai, S. L. (1986) *Arch. Biochem. Biophys. 244*, 50–56.

Bentley, K. L., Klebe, R. J., Hurst, R. E., & Horowitz, P. M. (1985) *J. Biol. Chem. 260*, 7250–7256.

Click, E. M., & Balian, G. (1985) *Biochemistry 24*, 6685–6696.

Cohler, L. F., Saba, T. M., Lewis, E., Vincent, P. A., & Charash, W. E. (1987) *J. Appl. Physiol. 63*, 623–633.

Dayhoff, M. O., Barker, W. C., & Hunt, L. T. (1983) *Methods Enzymol. 91*, 524–545.

Deno, D. C., McCafferty, M. H., Saba, T. M., & Blumenstock, F. A. (1984) *J. Clin. Invest. 73*, 20–34.

Ehrismann, R., Roth, D. E., Eppenberger, H. M., & Turner, D. C. (1982) *J. Biol. Chem. 257*, 7381–7387.

Freire, E., & Biltonen, R. L. (1978a) *Biopolymers 17*, 463–479.

Freire, E., & Biltonen, R. L. (1978b) *Biopolymers 17*, 481–496.

Freire, E., & Biltonen, R. L. (1978c) *Biopolymers 17*, 497–510.

Fukada, H., Sturtevant, J. M., & Quiocho, F. A. (1983) *J. Biol. Chem. 258*, 13193–13198.

Go, N. (1983) *Annu. Rev. Biophys. Bioeng. 12*, 183–210.

Hayashi, M., & Yamada, K. M. (1981) *J. Biol. Chem. 256*, 11292–11300.

Hayashi, M., & Yamada, K. M. (1982) *J. Biol. Chem. 257*, 5263–5267.

Hormann, H., & Seidl, M. (1980) *Hoppe-Seyler's Z. Physiol. Chem. 361*, 1449–1452.

Hynes, R. (1985) *Annu. Rev. Cell Biol. 1*, 67–90.

Ingham, K. C., Brew, S. A., Broekelmann, T. J., & McDonald, J. A. (1984) *J. Biol. Chem. 259*, 11901–11907.

Jackson, W. M., & Brandts, J. F. (1970) *Biochemistry 9*, 2295–2301.

Jilek, F., & Hormann, H. (1979) *Hoppe-Seyler's Z. Physiol. Chem. 360*, 597–603.

Johansson, S., & Hook, M. (1980) *Biochem. J. 187*, 521–524.

Keski-Oja, J., & Yamada, K. M. (1981) *Biochem. J. 193*, 615–620.

Klebe, R. J., Hall, J. R., Rosenberger, P., & Dickey, W. D. (1977) *Exp. Cell Res. 110*, 419–425.

Kleinman, H. K., Klebe, R. J., & Martin, G. R. (1981) *J. Cell Biol. 88*, 473–485.

Kornblihtt, A. R., Umezawa, K., Vibe-Pedersen, K., & Baralle, F. E. (1985) *EMBO J. 4*, 1755–1759.

Koteliansky, V. E., Glukhova, M. A., Benjamin, M. V., Smirnov, V. N., Filimonov, V. V., Zalite, O. M., & Venyaminov, S. Y. (1981) *Eur. J. Biochem. 119*, 619–624.

Krystek, S. R., Jr., Dias, J. A., Reichert, L. E., Jr., & Andersen, T. T. (1985) *Endocrinology (Baltimore) 117*, 1125–1131.

Manly, S. P., Matthews, K. S., & Sturtevant, J. M. (1985) *Biochemistry 24*, 3842–3846.

Mosesson, M. W., & Umfleet, R. A. (1970) *J. Biol. Chem. 245*, 5728–5736.

Mosesson, M. W., Chen, A. B., & Huseby, R. M. (1975) *Biochim. Biophys. Acta 386*, 509–524.

Mosher, D. F. (1984) *Annu. Rev. Med. 35*, 561–575.

Petersen, T. E., Thogersen, H. C., Skorstengaard, K., Vibe-Pedersen, K., Sahl, P., Sottrup-Jensen, L., & Magnusson, S. (1983) *Proc. Natl. Acad. Sci. U.S.A. 80*, 137–141.

Ploplis, V. A., Strickland, D. K., & Castellino, F. J. (1981) *Biochemistry 20*, 15–21.

Privalov, P. L. (1979) *Adv. Protein Chem. 33*, 167–241.

Privalov, P. L. (1982) *Adv. Protein Chem. 35*, 1–104.

Privalov, P. L., Mateo, P. L., Khechinashvili, N. N., Stepanov, V. M., & Revina, L. P. (1981) *J. Mol. Biol. 152*, 445–464.

Rourke, F. J., Blumenstock, F. A., & Kaplan, J. E. (1984) *J. Immunol. 132*, 1931–1936.

Ruoslahti, E., Engvall, E., & Hayman, E. G. (1981) *Collagen Relat. Res. 1*, 95–128.

Ryder, K. W., Kaplan, J. E., & Saba, T. M. (1975) *Proc. Soc. Exp. Biol. Med. 149*, 163–167.

Saba, T. M. (1982) *Prog. Liver Dis. 7*, 109–131.

Saba, T. M., Filkins, J. P., & Di Luzio, N. R. (1966) *J. Reticuloendothel. Soc. 3*, 398–414.

Saba, T. M., Blumenstock, F. A., Shah, D. M., Kaplan, J. E., Cho, E., Scovill, W., Stratton, H., Newell, J., Gottlieb, M., Sedransk, N., & Rahm, R. (1984) *Ann. Surg. 199*, 87–96.

Saba, T. M., Blumenstock, F. A., Shah, D. M., Landaburu, R. H., Hrinda, M. E., Deno, D. C., Holman, J. M., Cho,

E., Dayton, C., & Cardarelli, P. M. (1986) *Am. J. Med. 80*, 229-240.
Sekiguchi, K., Hakomori, S., Funahashi, M., Matsumoto, I., & Seno, N. (1983) *J. Biol. Chem. 258*, 14359-14365.
Skorstengaard, K., Jensen, M. S., Sahl, P., Petersen, T. E., & Magnusson, S. (1986) *Eur. J. Biochem. 161*, 441-453.
Stathakis, N. E., & Mosesson, M. W. (1977) *J. Clin. Invest. 60*, 855-865.
Sturtevant, J. M. (1974) *Annu. Rev. Biophys. Bioeng. 3*, 33-51.
Thomas, L., Smith, R. T., & VonKorff, R. W. (1954) *Proc. Soc. Exp. Biol. Med. 86*, 813-819.
Wallace, D. G., Donovan, J. W., Schneider, P. M., Meunier, A. M., & Lundblad, J. L. (1981) *Arch. Biochem. Biophys. 212*, 515-524.
Yamada, K. M. (1983) *Annu. Rev. Biochem. 52*, 761-799.
Yamada, K. M., & Olden, K. (1978) *Nature (London) 275*, 179-194.
Yamada, K. M., Kennedy, D. W., Kimata, K., & Pratt, R. M. (1980) *J. Biol. Chem. 255*, 6055-6063.

NMR Study of the Solution Conformation of Rat Atrial Natriuretic Factor 7-23 in Sodium Dodecyl Sulfate Micelles

E. T. Olejniczak,* R. T. Gampe, Jr., T. W. Rockway, and S. W. Fesik*
Pharmaceutical Discovery Division, Abbott Laboratories, Abbott Park, Illinois 60064
Received February 23, 1988; Revised Manuscript Received May 16, 1988

ABSTRACT: The conformation of the cyclic portion (7-23) of naturally occurring rat atrial natriuretic factor, ANF(1-28), has been examined in sodium dodecyl sulfate (SDS) micelles using high-resolution NMR techniques. Evidence is presented which shows that ANF(7-23) has several regions of definable structure in SDS micelles which were not observed in earlier studies in bulk solvents. The ^{1}H NMR resonances of ANF(7-23) in SDS micelles were assigned using sequential assignment techniques, and the conformational properties were analyzed primarily from proton-proton distances obtained from the quantitative analysis of two-dimensional nuclear Overhauser effect spectra. Three-dimensional structures consistent with the NMR data were generated by using distance geometry and constrained minimization/dynamics. Several similar but not identical structures were found which adequately satisfied the NMR constraints. Although none of the structures adopted a standard secondary structure, the conformations of three different sections of the peptide, 8-13, 14-17, and 18-21, were nearly identical in all of the predicted structures when individually superimposed.

Atrial natriuretic factor (ANF) is a peptide hormone which exhibits natriuretic, vasorelaxant, and hypotensive activities (de Bold, 1985; Cantin & Genest, 1985; Sonnenberg et al., 1983). Considerable effort has been expended to develop therapeutically useful mimics of this peptide by synthesizing analogues with amino acid substitutions and deletions. These studies have helped define the amino acid residues important for eliciting a biological response. However, in order to fully understand the factors governing the biological activity of a peptide hormone and to mimic its function, it is necessary to know not only the peptide's important functional groups but also their relative spatial orientation when bound to its receptor.

Several attempts have been made to deduce the bioactive conformation of ANF. In one approach, hypothetical models for the biologically active conformation were proposed on the basis of the structure activity data. In one such study, the biological activity of a series of ANF analogues in which each amino acid was systematically replaced with its D enantiomer indicated that the residues between Phe-8 and Ile-15 had the largest effect on activity. Furthermore, point substitutions of D-Ala for Gly suggested that the conformation of the ANF ring consisted of multiple turns (Nutt & Veber, 1987). These data can be compared to predictions based on Chou-Fasman rules which predict that the bioactive conformation consists of helical regions with no β sheet (Flynn, 1985).

Molecular modeling techniques have also been used to probe the accessible conformation space of the peptide to identify conformational features which could be tested by the synthesis of specific ANF analogues. In one study, 11 different families of related low-energy structures of ANF were identified from a short dynamics run (D. H. J. Mackay, personal communication). However, it is clear that an even larger number of families of structures would be found from a much longer run (S. Burt and C. Hutchins, personal communication). Because of the number of possible conformations for this flexible molecule, it is difficult to determine the bioactive conformation by these methods without additional data.

Another approach is to determine the preferred solution conformation of ANF and test whether this is the biologically active conformation by synthesizing appropriate conformationally restricted analogues. However, several studies have found that due to the flexibility of the peptide no preferred conformation could be observed in bulk solvents (Fesik et al., 1985; Theriault et al., 1987). Even for ANF analogues in which proline was substituted for glycine in order to rigidify the structure, no preferred conformation was found (Gampe et al., 1988).

In this paper, the conformational properties of the cyclic portion (7-23)

$$\underbrace{C^{7}\text{-F-G-G-R}^{11}\text{-I-D-R-I}^{15}\text{-G-A-Q-S}^{19}\text{-G-L-G-C}^{23}} \quad (1)$$

0006-2960/88/0427-7124$01.50/0